CORE
Metadata, citation and similar papers at core.ac.uk
Provided by Elsevier - Publisher Connector

ELSEVIER

Vailable online at www.sciencedirect.com

SciVerse ScienceDirect

Energy Procedia 27 (2012) 122 – 128

Energy Procedia

SiliconPV: April 03-05, 2012, Leuven, Belgium

High Throughput Ion-Implantation for Silicon Solar Cells

H. Hieslmair*, L. Mandrell, I. Latchford, M. Chun, J. Sullivan, B. Adibi

Intevac Corporation, Santa Clara, California

Abstract

Ion implantation is a technique that has been demonstrated to improve solar cell efficiency and eliminate process steps in standard and advanced cell designs. Intevac has developed a high productivity, continuous flux ion implantation tool for solar cells. We demonstrate improved n-type emitters over $POCl_3$ diffused emitters, and selective patterning capabilities. Additionally, it is shown that non-mass analyzed implantation provides similar performance as mass-analyzed implantation, yet at a much lower capital cost.

© 2012 Published by Elsevier Ltd. Selection and peer-review under responsibility of the scientific committee of the SiliconPV 2012 conference. Open access under CC BY-NC-ND license.

Keywords: ion implantation; selective emitter; non-mass analyzed

1. Introduction

Solar energy has emerged in the past five years to become a large and global industry. Worldwide PV market installations reached 27.4GW in 2011. The overall scale and the competitive nature of the solar industry has resulted in dramatic cost reductions in solar materials and manufacturing processes. Cost reductions will continue with an increasing amount of innovation in new processing techniques that will drive module efficiencies higher and total installation costs of solar power lower. Solar manufacturers will implement the most innovative process changes that provide maximum efficiency gains and cost reductions with minimal line disruption. Tools and technologies adopted today must not only meet today's $/W improvements, but must be extensible and compatible with the next improvements throughout a manufacturer's development roadmap. While roadmaps differ, there is a common focus in the immediate term on emitter improvements including better uniformity and blue light response, and selective emitters. In the longer term, the focus turns to B-BSF and various passivated rear structures, n-type wafers with boron emitters, and/or, PERC or PERL cells, and even IBC cells. Today's investments

* Corresponding author: hhieslmair@intevac.com

1876-6102 © 2012 Published by Elsevier Ltd. Selection and peer-review under responsibility of the scientific committee of the SiliconPV 2012 conference. Open access under CC BY-NC-ND license.
doi:10.1016/j.egypro.2012.07.039

in processes that improve emitters, need to also have a role in the subsequent cell architectures as well. Ion-implantation is one such technology that is extensible to advanced cell architectures.

Currently, the solar industry uses a thermal phosphorus diffusion process to form the emitters in the silicon cell which are not amenable to one sided and patterned emitter formation. Furthermore, there are issues with boron diffusion such as the formation of a boron rich layer (BRL) [1]. All of these issues hinder the industrial development of new and improved cell designs mentioned above.

An industrially viable ion-implantation solution would solve these issues, and provide a path to the industrial realization of higher efficiency cell designs. In the short term, ion-implantation could already assist with better dopant uniformity at higher sheet resistances, tailoring of profiles for reduced recombination (J_{0E}), [2, 3] the ability to passivate with thin oxide, and the elimination of PSG etch and edge isolation. These improvements can provide up to 0.4% to 1% in absolute efficiency improvement over diffused emitters.[4]

2. Examples of Implant in Silicon PV

One of the earliest references of using ion implantation for solar cells was in 1964 by King and Burrill [5]. King et al used a Van de Graff electrostatic accelerator to accelerate boron or phosphorus ions generated by an microwave ion source. More recently, numerous groups have shown high cell efficiencies using modern commercial mass analyzed (MA) implanters for both B and P implantations.[4,6,7]

Non-mass analyzed (NMA) implanters exhibit higher throughputs and lower capital costs. Glow discharge plasma source designs were common in the 1970's and 1980's.[8,9,10,11] A variety of dopant gasses including BF_3, B_2H_6, PH_3 and PF_5 were utilized as the precursors. One of the most advanced and ambitious implementations of implantation for solar cells was that by the Hoxan Corporation in Japan in 1982.[12] Using 4" round wafers, Hoxan built an integrated in-line, computer controlled, 9 megawatt manufacturing line utilizing: 1) NMA implanter using BF_3 (40keV) to form the rear B-BSF, 2) NMA implanter using solid P source (25keV) to form the emitter, 3) halogen lamp annealing, 4) TiO_2 ARC, 5) screen print, 6) firing, 7) tabbing & stringing and 8) module assembly & lamination. Each process was synchronized to 5 seconds per wafer for a 720 wph throughput.

Later, in 1987, using a glow discharge source, Wood et. al. [13] demonstrated 19.5% efficiency (AM1.5) using a NMA B_2H_6 (5% in H_2) implant for the emitter (n-type wafer) and a NMA PH_3 (1%in H_2) implant for the P-BSF. Using oxide passivation and photolithography to pattern evaporated metal contacts, they demonstrated >660mV Voc. The high Voc obtained by Wood et. al. demonstrates the exceptional quality of the implanted emitter and BSF and indicates that the co-implanted hydrogen was not deleterious despite the dilution of the dopant gas in H_2.

3. ENERG*i*™ ICP Source High Throughput Implanter

Intevac has developed a high throughput, continuous flux implanter. The Intevac ENERG*i* implanter and a schematic of the source design is shown in Fig. 1a and b. A large area inductively coupled plasma of any dopant bearing gas can be used. In this work, phosphine gas, PH_3, is employed to generate various charged species which can include PH_2^+, PH^+, P^+, H^+, and P_2H^+. The specific ratios of these radicals depends on the plasma pressure and RF power used. The grids at the bottom of the source chamber form a triode which accelerate these NMA species toward the wafer. In contrast to plasma immersion implantation, this architecture can provide a wide range of acceleration energies up to 100keV while maintaining low costs by using inexpensive DC high voltage power supplies instead of pulsed high voltage power supplies. Another advantage of this design is that a high beam current is maintained even

at low implant energies which is difficult for MA implanters. The ENERGi tool high throughput tool is designed for 2400 wph and will have three rows of wafers passing through three sections of an ion beam as illustrated in Fig. 1b. The motion through the ion beam assists in obtaining excellent dopant uniformity. Metal contamination is controlled by utilizing semiconductor grade graphite liners on all the internal surfaces of the tool and semiconductor purity feedstock gasses. Cell lifetimes derived from IQE measurements showed no degradation or slight improvement relative to $POCl_3$ emitters, indicating that metal contamination is not an issue (see 4.2 Cell Results).

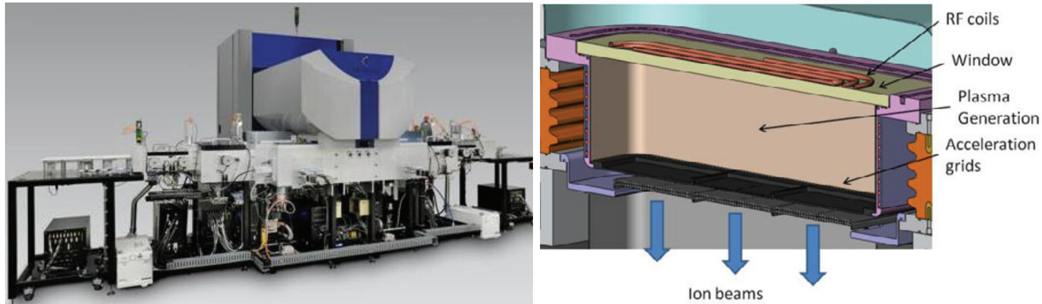

Fig. 1. Schematic of the in-line high throughput implantation tool (a) and the diagram of the source (b) featuring 3 wafer beams implanting 3 columns of wafers as they are passed underneath.

While this tool is recently operational, the work presented here was performed on a earlier prototype implantation tool. This tool is based on the same type of ICP PH_3 source with similar grids that form a triode to accelerate the ions. However, in the prototype tool, the wafer is static and the beam switched on and off such that the interval determines the dose. The beam itself can be seen in Fig. 2a covering a ~180 x 180mm area. This tool has demonstrated dose rates well in excess of $3x10^{15}$ $P/cm^2/s$, validating the high throughput capability of this design. Such a prototype tool is also being used to research boron implants using BF_3 plasmas.

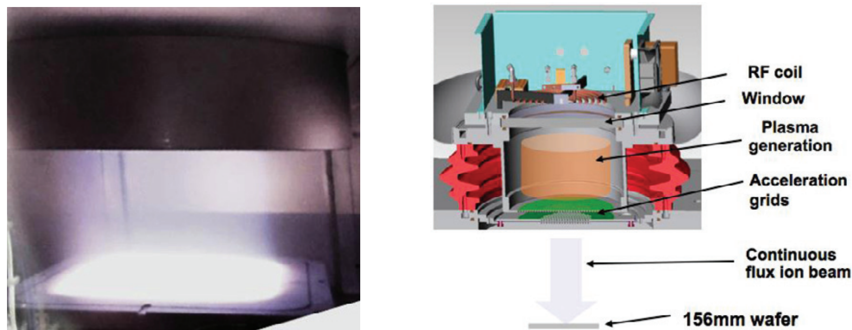

Fig. 2. View of the prototype static implanter ion beam (a) covering 156mm x 156mm wafer, and schematic of the prototype tool in (b).

As discussed earlier, further improvements in cell efficiency can be obtained by patterning of the dopants to form selective emitters. This has been demonstrated in the high throughput tool (Fig. 1) by placing a shadow mask in close proximity to the passing wafers. The ion beam covers the shadow mask which itself consists of sections. The one section of the shadow mask is a rectangular window which allows for the blanket implant as the wafer passes underneath. Another section of the shadow mask has narrow slot openings in the direction of wafer travel for the selective emitter implant. Thus with one pass,

both the blanket emitter (70 to 120 Ω/) as well as the selective emitter lines (40 to 60 Ω/) are formed. This provides a compelling capital and COO in comparison to other selective emitter methods. Additionally, such doped lines are also useful in other cell designs such as IBC.

4. Non-Mass Analyzed Implants

4.1. Profiles and Amorphization

The NMA implanted P SIMS profiles do differ from those of MA implants as shown in Fig. 3a. In particular, there are more species which have a shallower range than in MA implants. The result is a monotonically decreasing profile. During implantation, an amorphous surface layer is formed as damage is accumulated by the stopping of the incoming ions. During the anneal, the amorphous layer will recrystallize epitaxially starting from any a-Si/c-Si interface. Because of the lower P concentration near the surface in MA implants, it is possible to form a buried amorphous layer when targeting lighter doses for >100 Ω/ emitters. Buried amorphous layers have been shown to recrystallize poorly since the recrystallization proceeds from both the a-Si/c-Si interfaces and leaves a layer of defects where the recrystallizing interfaces meet. The NMA implants pose no risk of forming a buried amorphous layer because of the higher concentrations near the surface.

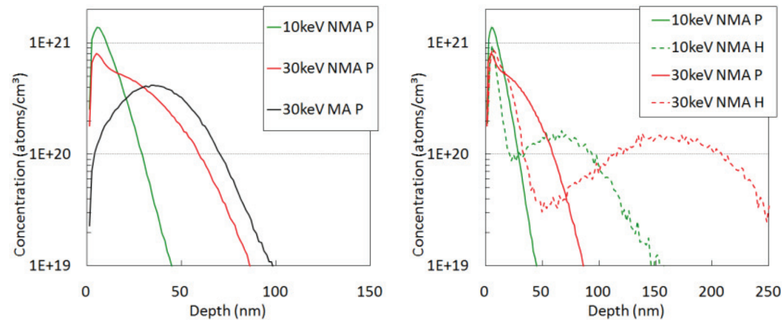

Fig. 3. SIMS profiles of non-mass analyzed (NMA) implantations from PH_3 plasma at 10keV and 30keV. The left graph compares NMA with MA at 30keV and the right graph shows the H^+ co-implantation profiles from the PH_3 implants.

Hydrogen is also co-implanted and H^+ profiles are shown in Fig. 3b. The SIMS P dose is approximately equal to the SIMS H dose. The implanted hydrogen does not appear to have deleterious effects. This is reflected in the literature based on J_{0E} measurements [2] and Voc [13] results as well as results presented here. It is expected that during annealing, the implanted hydrogen will diffuse out of the sample, and the small concentration of point defects created by H^+ implantation will anneal out. While there is often concern about residual ion-implant damage, there is also evidence that industrial $POCl_3$ and H_3PO_4 emitters have damage near the PSG/Si interface as well. [14, 15]

The residual implant damage after annealing is greatly dependent on the quality of the amorphized layer and the smoothness of the a-Si/c-Si interface.[16] Both aspects impact the quality of the epitaxial regrowth from the a-Si/c-Si interface. It has been shown that amorphization is improved by continuous and high fluxes of ions which are implanted at reduced temperatures.[17] In most other ion-implantation tools, the ion flux at a point on the wafer is effectively pulsed as the beam is rastered across the wafer. In the ENERG*i* implant tool, the wafer remains below 60°C during the continuous flux implant, helping to achieve a high quality amorphized layer even at lower doses suitable for >100 Ω/ emitters.

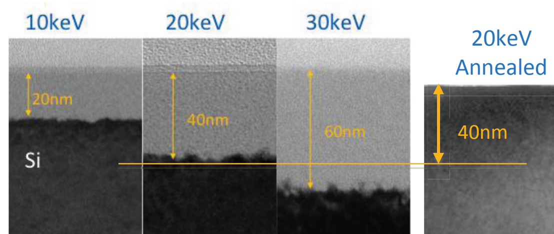

Fig. 4. TEM images showing amorphization depths of various energies for doses of 1.5 to $3x10^{15}$ P/cm^2. Also shown is TEM of the 20keV sample after anneal with no observable defects in the re-grown amorphized layer.

Fig. 4 shows TEM images of amorphized layers from NMA implantation of P at various energies. As the implant energy increases, the depth of the amorphized layer also increases. However, for energies less than 10keV, several effects need to be considered. One is an increase in sputtering rate of the surface. This becomes problematic for <2keV implants where the increased sputter rate begins to remove the implanted dose. Furthermore, during the anneal, some of the dose will be evaporated and/or lost in an oxide. This is exacerbated as the implant becomes shallower. An implant <5keV will require a significantly higher dose to maintain the same sheet resistance after anneal than a 20keV implant. Additionally, uniformity can become more difficult for low energy shallow implants if the final incorporated dose becomes more sensitive to local annealing conditions of the wafer and boat.

4.2. Cell Results

A group of 156mmx156mm pseudo-square mono-crystalline Si wafers were fabricated into solar cells using a standard cell line optimized for multi-crystalline wafers with 60 Ω/ $POCl_3$ emitters and rear Al-BSF. The line consisted of Centrotherm low pressure $POCl_3$ furnace, Rena wet rear and isolation etch, Centrotherm PECVD SiN_x, Baccini and Despatch printers and firing tools. One group of mono-crystalline wafers were passed through $POCl_3$ diffusion for the emitter formation. The other group was implanted in the prototype implanter and annealed at Intevac. Both groups were then processed simultaneously through the rest of the line (post-$POCl_3$). An efficiency improvement of 0.3% (absolute) was observed over the $POCl_3$ emitters as shown in Table 1. The gain in efficiency was primarily due to an improvement in V_{oc} to 630mV with the NMA emitters. The prototype static implanter has a known dose loss near the corners of the wafers, which degrades the FF. When wafers from both groups were cut down to 125mm x 125mm, then the efficiency improvement of the implant over the $POCl_3$ wafers widened to >0.5%. This non-uniformity at the corners does not exist on the in-line high volume tool as can be seen in the sheet resistance map in Fig. 5a, demonstrating a uniformity of 2.2% (1 sigma/mean = 1 contour).

Table 1. Improvement in cell performance by emitters from the prototype static implant tool vs a low pressure $POCl_3$ diffusion.

	Eta	Voc	Jsc	FF
156mm x 156mm	+0.33	+12.40	+0.27	-0.68
125mm x 125mm	+0.57	+14.21	+0.34	+0.09

The IQE results from finished cells of this study are shown in Fig. 5b, and demonstrate improved blue light response over $POCl_3$ emitter. Even with surface phosphorus concentrations suitable for Ag pastes (>$3x10^{20}$ P/cm^3), implanted homogenous emitters still tend to have better blue response for similar sheet resistances to diffused emitters as shown in Fig. 5b. The red IQE line is from the standard 60 Ω/ $POCl_3$ diffusion. The blue (NMA) and the gray (MA from [15]) IQE results are also 60 Ω/ and both show an improvement over $POCl_3$ emitter. No discernable difference is observed between the NMA and the MA

emitters, indicating that the extra H^+ implantation had no deleterious effects. Additionally, the cell lifetime determined from the IQE response [18], show no degradation from the NMA implants, indicating no relevant metal contamination.

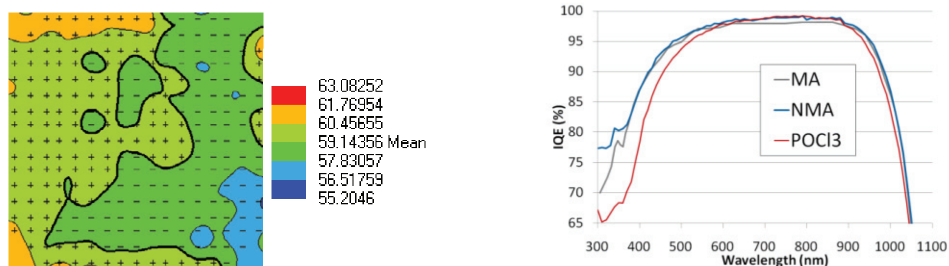

Fig. 5. a) A sheet resistance map illustrating a 2.2% uniformity (1 sigma/mean) from the in-line production tool in Fig. 1. The contour interval is 1 sigma/mean. b) IQE comparison of 60 ohm/sq emitters.

References

[1] M. A. Kessler, et al., Characterisation and implications of the boron rich layer resulting from open-tube liquid source BBr_3 boron diffusion processes, Proceedings of the *34th IEEE Photovoltaic Specialists Conference*, Philadelphia PA, 2009.

[2] H. Hieslmair, L. Mandrell, M. Chun, I. Latchford, and B. Adibi, Advantages of Ion-Implantation for Solar Cells, Proceedings of the *26th EuPVSEC*, Hamburg, Germany, 2011, pp. 1252-1256

[3] T. Ohrdes, et al., Solar cell emitter design with PV-tailored implantation, *Energy Procedia,* vol. 8, pp. 167-173, 2011.

[4] V. Yelundur, et al. First Implementation of Ion Implantation to Produce Commercial Silicon Solar Cells, Proceedings of the 26th EuPVSEC, Hamburg, Germany, 2011, pp. 831-834

[5] W. J. King and J. T. Burrill, Solar Cells Produced by Ion Implantation Doping, Proceedings of the *4th Photovoltaic Specialists Conference*, Clevland OH, 1964.

[6] M. Jeon, J. Lee, S. Kim, W. Lee, and E. Cho, Ion implanted crystalline silicon solar cells with blanket and selective emitter, *Materials Science and Engineering: B,* 2011.

[7] M. Hermle, J. Benick, M.Rüdiger, N. Bateman, and S. W. Glunz, N-Type Silicon Solar Cells with Implanted Emitter, presented at the 26th EuPVSEC, Hamburg, 2011.

[8] R. Wichner, E. J. Charlson, Silicon Solar Cells Produced by Corona Discharge, *Journal of Electronic Materials,* vol. 5, 1976.

[9] J. Ponpon and P. Siffert, "Silicon solar cells made by ion implantation and glow discharge," Proceedings of, 1975, pp. 342-348.

[10] J. Muller and P. Siffert, "Low cost molecular ion implantation equipment," *Nuclear Instruments and Methods in Physics Research,* vol. 189, pp. 205-210, 1981.

[11] J. Muller, E. Courcelle, D. Salles, and P. Siffert, Multiple-beam ion implantation setup for large scale treatment of semiconductors, *Nuclear Instruments and Methods in Physics Research Section B: Beam Interactions with Materials and Atoms,* vol. 6, pp. 394-398, 1985.

[12] Y. Tahara, et al., High through put automated junction formation by ion implantation and halogen lamp anneal for 9MW production, Proceedings of, 1985, pp. 792-796.

[13] R. Wood, R. Westbrook, and G. Jellison Jr, Excimer laser-processed oxide-passivated silicon solar cells of 19.5-percent efficiency, *Electron Device Letters, IEEE,* vol. 8, pp. 249-251, 1987.

[14] A. Armigliato, et al., Characterization of the PSG/Si interface of H_3PO_4 doping process for solar cells, *Solar Energy Materials and Solar Cells,* 2011.

[15] A. Gupta, et al., High Efficiency Selective Emitter Cells Using In-Situ Patterned Ion-Implantation, presented at the 25th EuPVSEC, Valencia Spain, 2010.

[16] L. Pelaz, L. A. Marqués, and J. Barbolla, Ion-beam-induced amorphization and recrystallization in silicon, Journal of applied physics **96**, 5947, (2004)

[17] E. J. H. Collart, et al., Process Characterization Of Low Temperature Ion Implantation Using Ribbon Beam And Spot Beam On The AIBT iPulsar High Current, Proceedings of the *18th International Conference on Ion Implantation Technology IIT 2010*, Kyoto Japan, 2010, pp. 49-52.

[18] P. A. Basore, Extended spectral analysis of internal quantum efficiency, Proceedings of the *23rd IEEE Photovoltaic Specialists Conference*, Louisville, KY, 1993, pp. 147-152.